Chemical Physics 130 (1989) 409–417
North-Holland, Amsterdam

ABSOLUTE BALMER LINE AND NH(c $^1\Pi \rightarrow$ b $^1\Sigma^+$, 0–0) VIBRATIONAL BAND EMISSION CROSS SECTIONS FROM NH_3 MOLECULES EXCITED BY ELECTRON IMPACT☆

Jelena M. KUREPA, Mirjana D. TASIĆ and Zoran Lj. PETROVIĆ
Institute of Physics, P.O. Box 57, 11000 Beograd, Yugoslavia

Received 16 May 1988; in final form 19 September 1988

The absolute Balmer line emission cross sections are determined in the processes of the electron impact dissociative excitation of ammonia. The optical excitation functions measured for these lines were investigated in the energy range 50–500 eV and normalized by the He benchmark procedure. The molecular continuum contribution has been eliminated from the obtained data. After that, the measured data have been corrected with the collection efficiency factor F to compensate the loss of optical signal due to non-thermal energies of the H excited fragments. The results for kinetic energy distribution functions for the ammonia molecules have been used for the F determination. The optical emission cross sections are determined with the accuracy of ± 15%. The cross sections for the NH(c $^1\Pi \rightarrow$ b $^1\Sigma^+$, 0–0) vibrational band have also been determined with an accuracy of ± 25%.

1. Introduction

Many experimental techniques are being used to achieve a better understanding of dissociative processes in electron–molecule collisions, as well as of highly excited molecular states. They are: time-of-flight measurements, optical cross section measurements, translational spectroscopy techniques and mass spectrometry techniques [1–3]. This knowledge is also needed for the development of new laser systems, in the research of planetary and cometary atmospheres and of many other interdisciplinary problems. Using the technique of optical cross section measurements, our attention has been concentrated on the quantitative determination of molecular fragment light emission from the dissociative electron–molecule collision processes [4–6]. However, the complexity of such molecular processes and the difficulty in quantitative light emission determination have been recognized and often pointed out (see refs. [4–6]). Just to enumerate some of them once more, they are as the first ones: the proper elimination of uncertainties in gas concentration measurements and the application of the reliable radiometric standard [7]. Adopting the He benchmark light signal calibration procedure, these two problems could be overcome [4,8]. But, some other problems like the elimination of a possible molecular continuum contribution from the measured fragment emission and the loss in the signal of detected fragment associated with the escape of the fast excited fragments from the experimental setup viewing region, should be still considered.

In the dissociative electron–hydrogen experiments [8–11], the last two cited problems have been analyzed and partly taken into account. The molecular contribution in the vicinity of the measured fragment lines has been determined using the special interference filters [8,10], or measured [9,11] by the working procedure completely described in ref. [11]. Some analyses of the possible loss of the measured Balmer line emission, due to the fast H excited fragments escaped from the apparatus viewing region have been also given [8,10]. However, rough approximation has been used for the sublevel population of the investigated excited H states and the values of the kinetic energies of these fragments. Thus, the presented data [8,10] have not been practically

☆ This material is based on the work supported by the US–Yugoslav Joint Fund for Scientific and Technological Cooperation, in cooperation with NBS under the grant p.p. 583.

corrected for this effect. In the case of some more complex molecules as C_3H_8, C_3H_6, n-C_4H_{10} [5] and CH_3Cl [6], the obtained Balmer line emission has been corrected only for the loss of the optical signal due to the non-thermal energies of the H excited molecular fragments. For these corrections, the average kinetic energies of the corresponding H fragment data published in refs. [12–15] have been adopted.

The aim of this work is to investigate the absolute line emission cross sections for the Balmer line emission ($n=3, 4, 5, ..., 8 \rightarrow n=2$) from ammonia molecules, in the dissociative interaction processes with electrons in the energy range 50–500 eV. The main purpose is, firstly, to eliminate the possible continuum contribution from the investigated Balmer line emission, and secondly, to analyze the loss in measured Balmer line signals due to escape of the fast H excited fragments.

The ammonia molecule has been chosen to be investigated for the following reasons: (1) some Balmer line emission cross sections have been determined in the e–NH_3 interactions [16] with electrons of 100 eV and the cross section for Hα in the energy range 20–2000 eV; (2) very recently the absolute Balmer line emission cross sections from the NH_3 molecule have been published again [17] being in rather a disagreement with the results given in ref. [16]; (3) the translational-spectroscopy results concerning the kinetic energy distribution of the H excited fragments from ammonia have recently been determined [18,19]; (4) ammonia is a rather important molecule in the plasma processing, being a source of nitrogen atom for the deposition of nitride films. Our results for Balmer line emission have been determined as the absolute cross section data with the molecular continuum contribution eliminated. It has been achieved using the specially designed optical detection system [20]. To obtain the needed cross sections, the He benchmark normalization procedure [4,8] has been adopted for the calibration purposes of the measured optical excitation functions. Apart from the Balmer emission, our attention has also been devoted to the determination of the cross section of the NH($c\ ^1\Pi \rightarrow b\ ^1\Sigma^+$, 0–0) vibrational band emission.

The excitation functions measured for the Balmer line emission and the NH($c\ ^1\Pi \rightarrow b\ ^1\Sigma^+$, 0–0) band emission from the dissociative excitation of ammonia have been determined with a reproducibility of ±3–5% and 15% respectively. Since the He benchmark cross sections at normalization energy $E_n = 100$ eV have been obtained with the high confidence level of ±7%, the gas concentration measurements by a capacitance manometer have been conducted with the accuracy of ±1% and the electron current measurements better than ±1%, we have obtained the absolute emission cross sections with the accuracy of ±15% for Balmer line emission and ±25% for the NH($c\ ^1\Pi \rightarrow b\ ^1\Sigma^+$, 0–0) band emission.

2. Experimental

2.1. Apparatus

The apparatus used in this experiment practically consists of two parts: the experimental device already described in detail by Kurepa and Tasić [4] and the automatic spectroscopic photon counting detector system specially designed for our experiments [20]. The first part basically includes two differentially pumped vacuum chambers (background pressure of 10^{-4} Pa), one of them containing the electron gun, and the other one (interaction chamber) containing the four-element electron lens system [21] with a specially designed Faraday cup. Using a pair of Helmholtz coils, the earth and stray magnetic fields in both chambers have been reduced to the value of ≈3 mG. The working gas pressure in the interaction chamber (of the order of 0.1 Pa) has been measured by a capacitance manometer (MKS Baratron, model 77H-1), while the electron beam current has been of the order of 20 μA. The obtained optical emission has been observed from interaction chamber at an angle of 90° with respect to the electron beam. The optical detection system described in detail in ref. [20], basically contains the optical monochromator (Zeiss SPM-2) with the shaft encoder driven by the two-directional motor, the cooled photomultiplier (RCA 31034 C), the single-pulse counting system (ORTEC), the multichannel analyzer (Nuclear Data Series 2200 system analyzer) used in the multiscaling mode and a specially designed control unit. This unit is designed to control both the rotation of the optical monochromator shaft and the accumulation of the emitted photon pulses in the interval λ_1–λ_2 or λ_2–λ_1

nm. It activates the multichannel analyzer memory to feed the first group of 256 channels with the photon pulses corresponding to the shaft rotation from λ_1 to λ_2 nm. In the opposite direction, from λ_2 to λ_1, the multichannel analyzer memory feeds another group of 256 channels, too. The shaft rotation for spectral range λ_1–λ_2 or λ_2–λ_1 nm has been controlled electronically by the special relay and the two-directional motor. In the shaft direction λ_2–λ_1 nm, the electron voltage, by which the electron beam has been extracted from the thermoemitter, changes its sign, what actually stops the electron beam to get into the interaction chamber. The obtained optical signal is then only the background signal of the system. The difference between the signals from the first memory group and the second one presents the real signal from fragment emission and molecular emission in the λ_1–λ_2 nm interval. Using such automatic spectroscopic photon counting system, we have been able to investigate the chosen spectral interval with the desired optical resolution and the statistic accuracy, i.e. we could investigate molecular continuum spectra and – on the top – the atomic lines and the vibrational bands following dissociative electron–ammonia interactions.

The emission spectra of ammonia have been observed in the wavelength region of 374–700 nm. The gratings used in the monochromator were with the reciprocal dispersion of 4 nm/mm for 320–600 nm and 2 nm/mm for 400–700 nm wavelength range, respectively. The relative wavelength sensitivity has been measured for the whole detection system and the obtained curves for both regions of interest have been presented in ref. [5]. The investigated emission spectra have been analyzed for the electron energy interval of 50–500 eV successively.

2.2. Results

The emission spectra of the excited fragments in the electron–ammonia binary collision type of interaction in the spectral range of 374–700 nm are presented in fig. 1. It could be seen from fig. 1, that with the spectral resolution of the experiment, the Balmer lines originating from the $n=3, 4, 5, ..., 8$ levels are well resolved and could be simply detected. The position of the NH($c\ ^1\Pi \rightarrow b\ ^1\Sigma^+$, 0–0) vibrational band is marked and in spite of its rather weak emission, it is essentially properly resolved from the neighbouring atomic emission. The typical experimental result obtained in the multiscaling mode corresponding to 100 nm spectral interval is shown in fig. 2. This is the result of the optical emission in the 400–500 nm wavelength region for one electron beam energy, with the eliminated background signal. The molecular continuum contribution in this spectral range, as well as the Hβ, Hγ and Hδ lines are observed. Changing the electron beam energy, in the range 50–500 eV, under identical experimental conditions and for the same spectral range, we were able to determine the optical excitation functions for atomic lines (in $\Delta\lambda$ interval, see fig. 2) and molecular contribution excitation function in the same $\Delta\lambda$ interval. The atomic lines which have been studied from the result presented, for example, in fig. 2 are: Hβ, Hγ and Hδ lines. Changing the width of the measured spectral interval and its position in the spectra, we have measured the Hα, Hβ, Hγ, Hδ, Hε and Hξ excitation functions and the functions of the relevant molecular contributions.

To determine the low-signal NH($c\ ^1\Pi \rightarrow b\ ^1\Sigma^+$, 0–0) excitation function, a special effort has been invested in measuring, at the proper spectral position, the 25 nm spectral interval in the multiscaling mode. By the use of the standard three-point smoothing procedure to smooth the obtained data and by the numerical integration in the whole vibrational band (for each particular electron energy) its excitation function has been determined. Reproducibility of the data for the atomic excitation functions was 3–5%, while for the investigated NH vibrational band, it was 15%.

To normalize the excitation functions to the absolute emission cross sections, a standard He benchmark procedure [7] has been applied using two He transitions: 4 ^{1}S–2 ^{1}P for Hα, Hβ and Hγ and 5 ^{1}S–2 ^{1}P for Hγ, Hδ, Hε, Hξ and the NH($c\ ^1\Pi \rightarrow b\ ^1\Sigma^+$, 0–0) band. The adopted procedure for the calibration of the absolute emission cross sections has already been presented in detail elsewhere [5,6].

In table 1, the absolute emission cross section data for the ($n=3, 4, ..., 8 \rightarrow n=2$) Balmer lines are given, as well as for the NH($c\ ^1\Pi \rightarrow b\ ^1\Sigma^+$, 0–0) vibrational band. These data, obtained with the detection system described above, are without molecular continuum contribution and incorporate systematic errors due to the loss of the signal from the non-thermally ex-

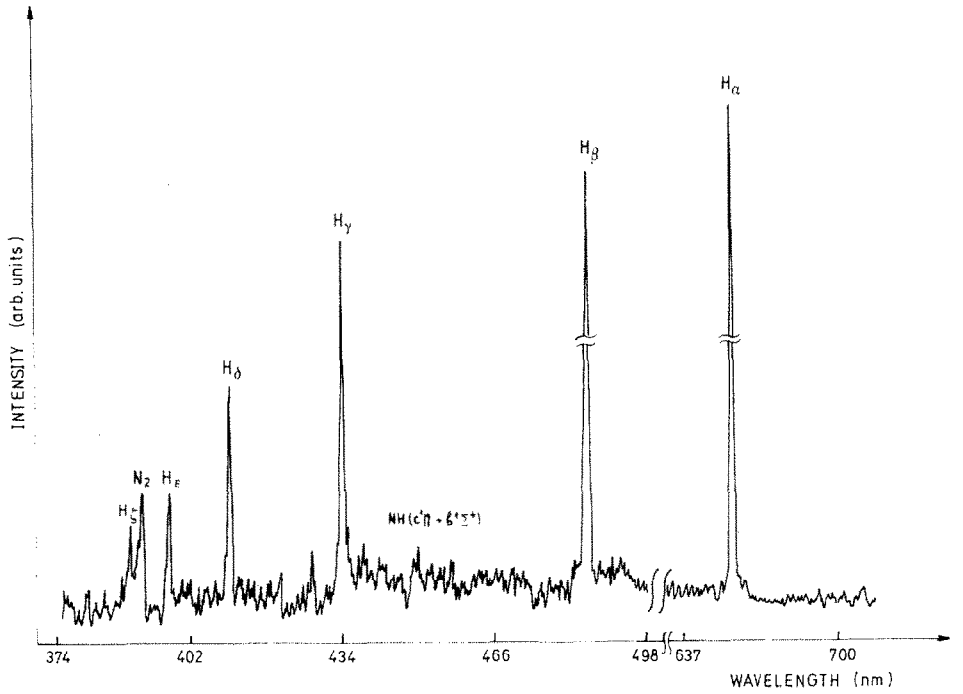

Fig. 1. Optical emission spectra of ammonia in the 374–700 nm region. Electron energy 100 eV, electron beam current 60 μA.

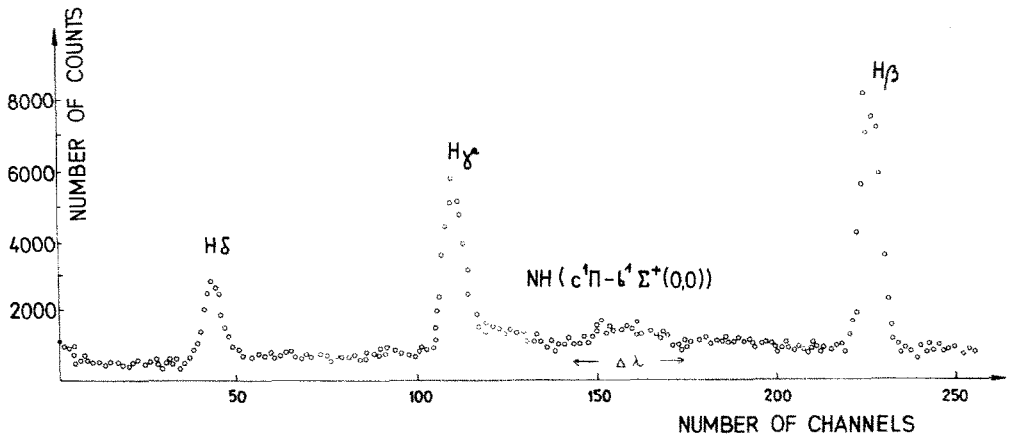

Fig. 2. Optical emission spectra of ammonia in the 400–500 nm region. Electron energy 100 eV.

cited H fragments. The analysis of this loss at 100 eV is given in section 3. The data given in table 1 are shown in figs. 3 and 4 and are compared with the results for 100 eV published in ref. [16].

In fig. 5, as an example, the cross sections for the Hδ line where molecular contribution has not been subtracted (curve a) are given. There are also given the corrected data for this contribution (curve b), and the relevant cross section function for the molecular continuum in that spectral domain (curve c).

In table 2, the molecular continuum contributions are presented to demonstrate how large they could be

Table 1
Balmer line and NH(c $^1\Pi \rightarrow b\ ^1\Sigma^+$, 0–0) vibrational band emission cross sections for ammonia (units of 10^{-22} m^2)

E (eV)	Hα	Hβ	Hγ	Hδ	Hϵ	Hξ	NH(c $^1\Pi \rightarrow b\ ^1\Sigma^+$, 0–0)
50	1.68	0.540	0.252	0.119	0.0551	0.0257	0.0416
60	3.35	0.703	0.323	0.145	0.0720	0.0334	0.0500
70	3.65	0.762	0.335	0.155	0.0773	0.0360	0.0500
80	3.81	0.818	0.355	0.157	0.0827	0.0386	0.0527
90	3.86	0.818	0.353	0.162	0.0835	0.0388	0.0511
100	3.76	0.810	0.345	0.153	0.0827	0.0384	0.0489
150	3.25	0.712	0.298	0.130	0.0728	0.0338	0.0435
200	2.59	0.513	0.235	0.103	0.0582	0.0272	0.0353
300	1.79	0.393	0.165	0.071	0.0391	0.0185	0.0261
400	1.48	0.327	0.132	0.063	0.0337	0.0154	0.0261
500	1.13	0.237	0.106	0.047	0.0245	0.0113	0.0188

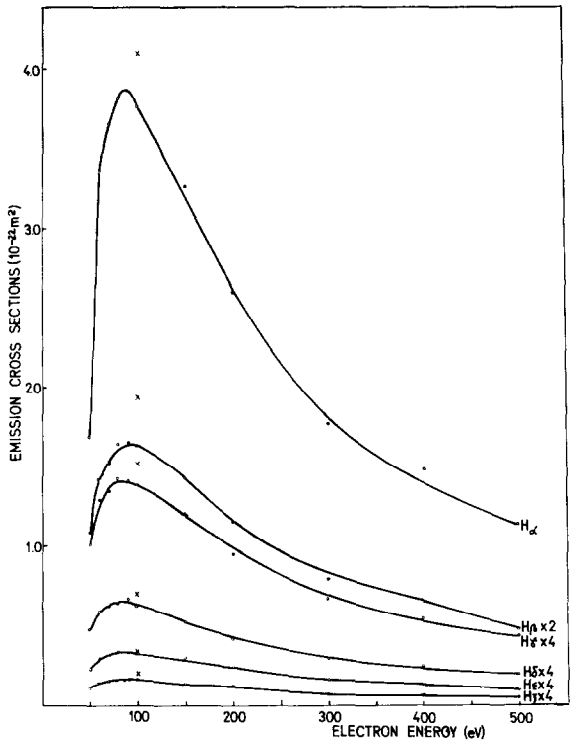

Fig. 3. Balmer line emission cross sections for ammonia corrected for molecular continuum contribution. (○) Present work, (×) ref. [6].

in the vicinity of the investigated Balmer lines at 100 eV.

3. Discussion

The excited fragments of the parent molecule dissociated in binary electron-impact processes, may have rather large kinetic energies. Consequently, a certain number of them leave the viewing region of the experimental setup before emitting a photon. The measured cross section is, therefore, smaller than the real cross section, since the contribution of the escaping fragments is not included in the measured signal. This is especially a serious problem for the long-lived excited states of the fragments.

The detailed description of the geometry of the electron–gas target region and the viewing region are required to correct the absolute emission cross sections for this effect. The general formulae for the light collection efficiency factor F has already been given and used [5,6]. This quantity F gives the percentage of the collected radiation and is given by

$$F = 1 - \frac{\operatorname{erf}(a/2\sigma + w/a) - \operatorname{erf}(a/2\sigma - w/a)}{2\left|\operatorname{erf}(a/2\sigma + w/a)\mathrm{e}^{w/\sigma} - \operatorname{erf}(a/2\sigma)\right|} \times \mathrm{e}^{-\Delta/\sigma}. \quad (1)$$

It is valid for a Gaussian electron beam where a is a numerical factor determined from the electron beam distribution ($a = 0.466w$).

$2w$ is the electron beam width, σ is the decay length defined as

$$\sigma = \tau V_y = \tau\sqrt{2\epsilon/M}\,\Psi. \quad (2)$$

Here τ is the lifetime of the upper level of the excited state, V_y is the velocity of the fragments along the y

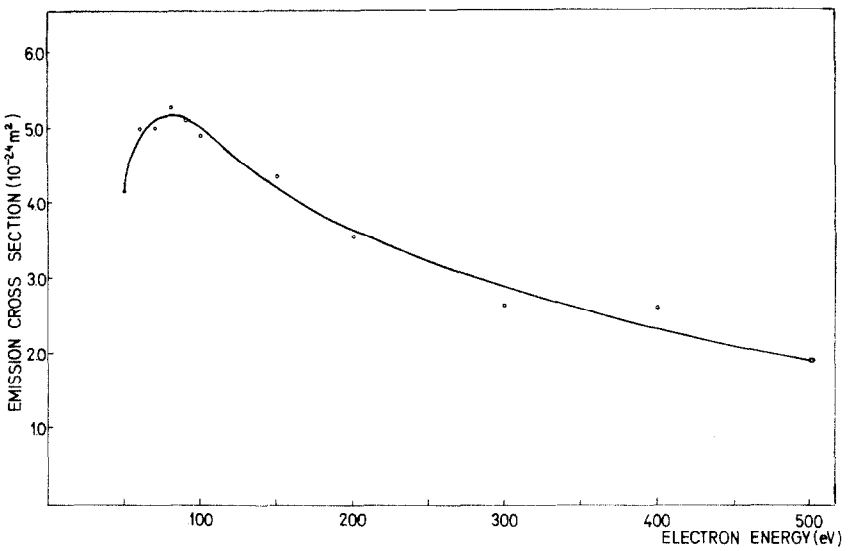

Fig. 4. Absolute emission cross section of the NH(c $^1\Pi \rightarrow$ b $^1\Sigma^+$, 0–0) vibrational band corrected for molecular continuum contribution.

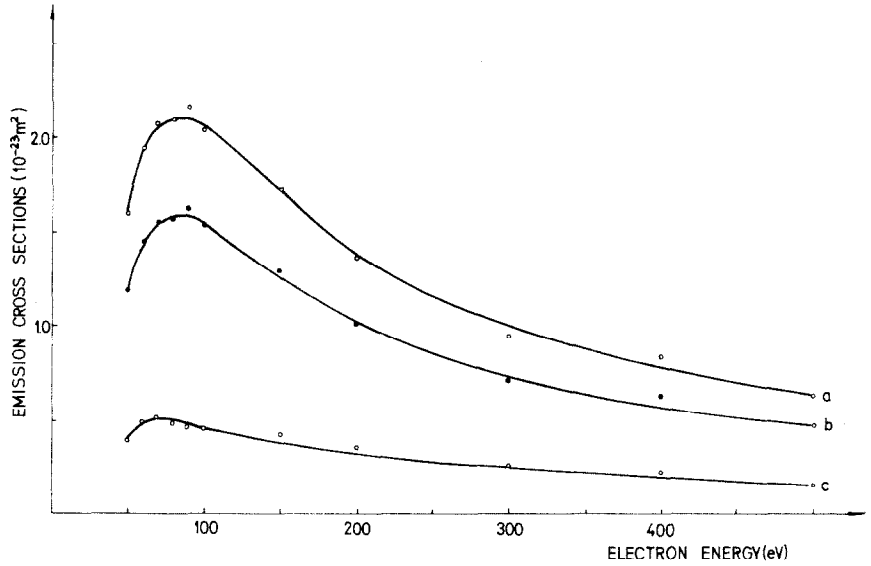

Fig. 5. Emission cross sections of the Hδ line. (a) Uncorrected data. (b) Data corrected for molecular continuum contribution. (c) Molecular continuum contribution cross section data.

axis (perpendicular to both the line of the sight and the electron beam), Ψ is a numerical factor describing the ratio between V_y and $V\,(=\sqrt{2\epsilon/M})$ and also includes effects of anisotropy of the EDF (kinetic energy distribution of excited fragments) (when EDF is isotropic, $\Psi=1/2$), 2Δ is the width of the observation region, determined practically by the height of the optical monochromator slit. The only way to average $F(\Delta, \epsilon)$ was to use the approximation

$$\langle F(\Delta, \epsilon)\rangle = F(\Delta, \langle \epsilon \rangle) = F, \tag{3}$$

as it has already been done in our previous publications [5,6]. However, the effective kinetic energies used in refs. [5,6] were obtained from the width at

Table 2
The molecular continuum contribution to the investigated Balmer line emission at 100 eV

Line	Molecular contribution (%)
Hα	0
Hβ	6
Hγ	14
Hδ	25
Hε	25
Hξ	65

half height of the Doppler profiles of the emitted radiation and could not adequately represent the contribution of the high-energy fragments which are most likely to escape the detection. In other words, a kinetic energy distribution function (EDF) of the H excited fragments is needed to determine the $\langle F(\Delta, \epsilon)\rangle = F$ correction. But, these functions (EDFs) could include several groups of fragments (see fig. 6, curve $f(\epsilon)$). Even though the average energy could be determined by the bulk of the distribution, F is mainly sensitive to the high-energy tail of EDFs (see $F_{n,s}$ in fig. 6). Therefore, obviously, the full kinetic energy distribution of the excited fragments under investigation is required to determine the proper correction for this effect. Such data have recently been available for some molecules including NH_3 [15,19]. To determine the values of F for Balmer lines from NH_3 more precisely than has been done in refs. [5,6] for other gases we have adopted the following approximation:

$$F(\Delta) = \langle F(\Delta, \epsilon)\rangle = \int_0^\infty F(\Delta, \epsilon) f(\epsilon)\, d\epsilon \qquad (4)$$

$$\left(\int_0^\infty f(\epsilon)\, d\epsilon = 1\right),$$

where $f(\epsilon)$ is the isotropic EDF.

In the present analysis the following approximations have been made which are very well justified by recent experimental observations [16,19].

(1) It is assumed that the EDFs for the Hα and Hβ lines are very similar to the EDFs for Hγ, Hδ, etc., as indicated by the observation in ref. [16].

(2) Since our apparatus cannot distinguish between the different excited H sublevels (s, p and d sublevels), effective factors $F_{n,\mathrm{eff}}$ were calculated for Balmer lines in ammonia, and presented in table 3. They have been obtained as consisting of sublevel escape factors F_{ns}, F_{np} and F_{nd} which have been calculated using experimentally determined populations of the sublevels given in ref. [22]. Practically, the results obtained in ref. [22] are valid only for the Hα line from NH_3 at 300 eV ($I_{3s}/I_{H\alpha}=0.26$, $I_{3p}/I_{H\alpha}=0$ and $I_{3d}/I_{H\alpha}=0.74$). In spite of this, such ratios have been used for all Balmer lines and for the electron energy of 100 eV, due to the fact that a few authors [22–24] have obtained that $I_{3s}/I_{H\alpha}$ ratio "is approximately independent of the electron impact energy" [23]. In fig. 6 we present the EDF ($f(\epsilon)$) of the Hβ line for 100 eV electrons incident on NH_3 molecules [19]. Also numerical calculations for the energy dependence of some $F_{n,s}$ values for our apparatus are given.

(3) The isotropy of the emitted fragment radiation is assumed for all Balmer lines, due to the practically zero values obtained for the polarization factor P (%) for the Hα line from the binary electron–ammonia interactions [16]. The polarization factor is also expected to be zero for other Balmer lines. In table 3, F_{ns}, F_{nd} and $F_{n,\mathrm{eff}}$ are presented but only $F_{n,\mathrm{eff}}$ values have been applied to correct the obtained Balmer cross sections (see table 4) at 100 eV. These corrections could be applied for the entire investigated energy range (50–500 eV) since measurements in ammonia [25] have shown that the $\bar{\epsilon}$ (eV) of the excited H fragments above 60 eV electron impact energy have been constant. Our results for the absolute Balmer line cross section at 100 eV are given in table 4, as well as the data from refs. [16,17]. They are presented as Q_m – the cross sections corrected for the

Table 3
Apparatus light collection efficiency factors F_{ns}, F_{nd} and $F_{n,\mathrm{eff}}$ for Balmer lines ($n=3, \ldots, 8$) from NH_3 at 100 eV

	F_{ns}	F_{nd}	$F_{n,\mathrm{eff}}$(s–d)
Hα	1	1	1
Hβ	0.97	1	0.99
Hγ	0.90	1	0.96
Hδ	0.80	1	0.93
Hε	0.68	0.99	0.90
Hξ	0.53	0.94	0.83

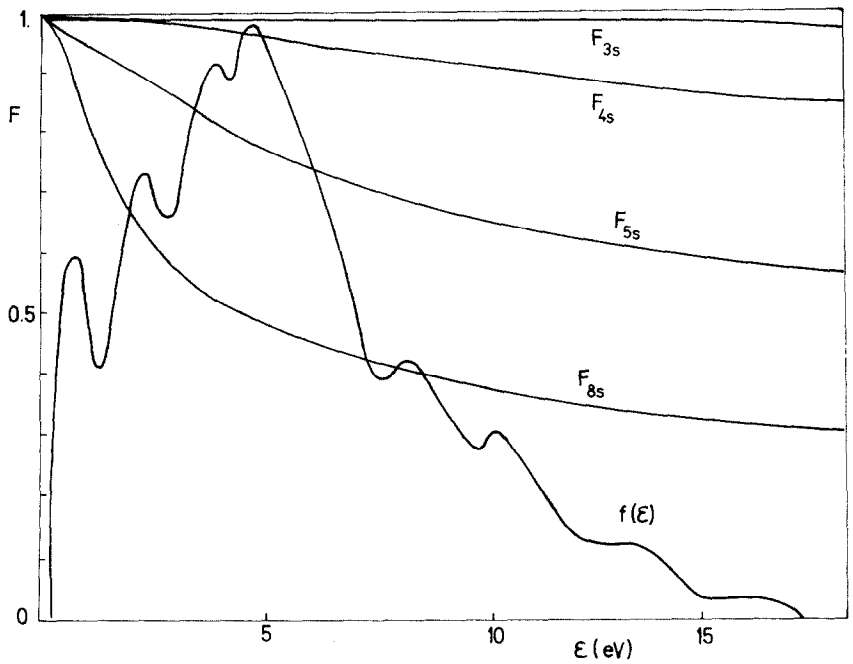

Fig. 6. Kinetic energy distribution function (EDF) of H* ($n=4$) fragments produced by dissociation of NH_3 [19]. Energy dependence of some F_{ns} values for the detection system used.

Table 4
Absolute emission cross sections Q_{em} (10^{-22} m^2) of Balmer radiation produced by electron impact on NH_3 at 100 eV

Line	Q_{em} (10^{-22} m^2)			
	present work		ref. [16]	ref. [17]
	Q_m [a]	Q_{mF} [b]		
Hα	3.76	3.76	4.11	2.20
Hβ	0.810	0.318	0.975	0.516
Hγ	0.345	0.359	0.381	0.206
Hδ	0.153	0.265	0.175	0.109
Hε	0.0827	0.0919	0.0857	0.0436
Hξ	0.0384	0.0463	0.0541	
Hτ			0.0208	0.0133
Hθ			0.0141	

[a] Cross sections corrected for molecular continuum contribution.
[b] Cross sections corrected for molecular continuum contribution and apparatus light collection efficiency $F_{n,eff}$.

molecular contribution – and Q_{mF} – the cross sections corrected for both the molecular contribution (negative correction) and the escape of the fast H fragments (with F_{eff}) (positive correction). From tables 2 and 3, it could be seen how large these corrections are for each Balmer line at 100 eV. Both types of correction are almost comparable and cancel each other for Hα, Hβ, and Hγ lines, but if not taken into account, they introduce systematic errors (higher cross section data) for Hδ, Hε, Hξ, etc. The results given in table 4 show that for the Hα line, where no correction is needed, our result is in very good agree-

ment with the result of ref. [16], while it is in disagreement with the result of ref. [17]. This is rather unexpected, since basically the same type of calibration procedure (the He benchmark calibration) has been applied in our experiment and the one described in ref. [17]. In the experiment in ref. [16], a different normalization method has been used, the so-called traditional method [26] which for the optical signal calibration purposes incorporates the standard tungsten ribbon lamp at a known temperature. Expected agreements of our results with the data given in ref. [16] have also been obtained for the other Balmer line emission cross sections. The existing difference is also expected since in ref. [16] no correction was applied. However, there is a general disagreement of up to 50% between both, our results and the data from ref. [16], and the recently published absolute Balmer cross sections from dissociative electron–ammonia interactions [17]. The reason for this disagreement is not clear at present. Generally the authors of ref. [17] have also found about 30% lower Balmer line cross section values in comparison with the data already reported for H_2, CH_4 and SiH_4 [5,8,16,27,28] which also has not been understood.

Acknowledgement

This work is partly financed by US–Yugoslav Joint Fund–NBS grant p.p. 583. We wish to note that we appreciate very much their support. We are also grateful to Dr. G.H. Dunn for his constant interest in our work, and also to Dr. T. Ogawa for sending us his data regarding kinetic energy distribution of H excited fragments from ammonia.

References

[1] R.N. Compton and J.N. Bardsley, Electron–molecule collisions, eds. I. Shimamura and K. Takayamagi (Plenum Press, New York, 1984) pp. 275–349.
[2] E.C. Zipf, Electron–molecule interactions and their applications, ed. L.G. Christophorou (Academic Press, New York, 1984) p. 335.
[3] Y. Hatano, Comments At. Mol. Phys. 13 (1983) 259.
[4] J.M. Kurepa and M.D. Tasić, Chem. Phys. 38 (1979) 361.
[5] J.M. Marendić, M.D. Tasić and J.M. Kurepa, Chem. Phys. 91 (1984) 273.
[6] J.M. Kurepa and J.M. Marendić, Fizika 16 (1984) 4, 327.
[7] B. van Zyl, G.H. Dunn, G. Chamberlain and D.W.O. Heddle, Phys. Rev. A 22 (1980) 1916.
[8] G.A. Khayrallah, Phys. Rev. A 13 (1976) 1989.
[9] C. Karolis and E. Harting, J. Phys. B 11 (1978) 357.
[10] R.S. Freund, J.A. Schiavone and D.F. Brader, J. Chem. Phys. 64 (1976) 1122.
[11] C. Karolis, Ph. D. Thesis, University of New South Wales, Australia (1977).
[12] N. Kouchi, K. Ito, Y. Hatano and T. Tsubai, Chem. Phys. 36 (1979) 239.
[13] N. Kouchi, M. Ohno, K. Ito, N. Oda and Y. Hatano, Chem. Phys. 67 (1982) 287.
[14] K. Ito, N. Oda, Y. Hatano and T. Tsubai, Chem. Phys. 21 (1977) 203.
[15] T. Ogawa, J. Kurawaki and M. Higo, Chem. Phys. 61 (1981) 181.
[16] G.R. Möhlmann and F.J. de Heer, Chem. Phys. 40 (1979) 157.
[17] T. Sato, F. Shibata and T. Goto, Chem. Phys. 108 (1986) 147.
[18] J. Kurawaki and T. Ogawa, Chem. Phys. 86 (1984) 295.
[19] T. Ogawa, private communication (1986).
[20] J.M. Kurepa, B.M. Panić, B.J. Levi, Spectrochim. Acta 32 B (1977) 413.
[21] M.V. Kurepa, M.D. Tasić and J.M. Kurepa, J. Phys. E 7 (1974) 940.
[22] S. Tsurubuchi, G.R. Möhlmann and F.J. de Heer, Chem. Phys. Letters 48 (1977) 477.
[23] G.R. Möhlmann, S. Tsurubuchi and F.J. de Heer, Chem. Phys. 18 (1976) 145.
[24] G.A. Khayrallah and S.J. Smith, Chem. Phys. Letters 48 (1977) 289.
[25] N. Kouchi, M. Ohno, K. Ito, N. Oda and Y. Hatano, The XIth ICPEAC, Kyoto, Japan (1979) p. 366.
[26] C.I.M. Beenakker and F.J. de Heer, Chem. Phys. 6 (1974) 291.
[27] J. Perrin and J.F.M. Aarts, Chem. Phys. 80 (1983) 351.
[28] T. Sato and T. Goto, Japan. J. Appl. Phys. 25 (1986) 937.